

Angiogenesis in residual cancer and roles of HIF-1 α , VEGF, and MMP-9 in the development of residual cancer after radiofrequency ablation and surgical resection in rabbits with liver cancer

H. Li, B. Zhao, Y. Liu, W. Deng, Y. Zhang

Department of Ultrasound, The First Hospital Affiliated to Inner Mongolia Medical University, Hohhot, People's Republic of China

[Received: 21 April 2019; Accepted: 25 April 2019]

Background: The aim of the study was to investigate the changes of blood flow signal in residual cancer after ultrasound-guided radiofrequency ablation (RFA) treatment of rabbit liver cancer over time, and to analyse the correlation between changes in blood flow signal and changes in hypoxia-inducible factor 1-alpha (HIF-1 α), vascular endothelial growth factor (VEGF), and matrix metalloproteinase-9 (MMP-9) in residual cancer tissue after RFA.

Materials and methods: One hundred and ten rabbits were randomly selected, VX2 tumour cells were implanted subcutaneously, tumour cells were implanted in liver. Ninety rabbits were divided into three groups: Group 1 — untreated controls, Group 2 — RFA group, Group 3 — surgical resection group. Tumour size, blood flow signal, microvessel density (MVD) in liver cancer were assessed.

Results: Correlation of HIF-1 α , VEGF, MMP-9 mRNA and protein expressions with blood flow signal in residual cancer were observed. Liver tumour was 2.3 ± 0.32 cm, significant differences in the grade of blood flow signal were noted among different time points (days 0, 3, 7, and 14; $p < 0.05$). Significant differences were also observed between the surgical resection and RFA groups at the same time points ($p < 0.05$). The MVD in the RFA group was lower than that in the control group, but higher than that in the surgical resection group. The immunohistochemical scores for VEGF and MMP-9 in the RFA group were lower than those in the control group, but higher than those in the surgical resection group. The grade of ultrasound blood flow signal was positively correlated with the expression of two angiogenesis-related factors, VEGF and MMP-9, and the MVD in the control, RFA, and surgical resection groups.

Conclusions: There is a higher risk of tumour recurrence with RFA than with surgical resection. (Folia Morphol 2020; 79, 1: 71–78)

Key words: radiofrequency ablation, HIF-1 α , VEGF, MMP-9, liver cancer

INTRODUCTION

Primary liver cancer, especially hepatocellular carcinoma, is a prevalent disease with a world-wide incidence of 1 million new cases each year. However, surgery is indicated only in 10% to 30% of the cases [1]. Clinical studies have found that ultrasound-guided radiofrequency ablation (RFA) can control liver cancer and relieve the symptoms to some extent [2]. However, it is difficult to achieve overall inactivation with RFA for large-diameter tumours. Although simultaneous multi-point ablation is an option, the mechanisms of neovascularisation, recurrence, and metastasis of residual tumour have not been fully understood. It has been reported that RFA can induce hypoxia and significantly increased angiogenesis in surrounding surviving tissue while destroying tumour tissue.

Previous studies have focused on the relationship between microvessel density and matrix metalloproteinase-9 (MMP-9) or the pathological changes after RFA over a short observation period (24 h) [3]. No studies have continuously observed the changes of blood flow signal in liver cancer after RFA over a long period (2 weeks), and analysed the correlation between such changes and the dynamic changes of hypoxia-inducible factor 1- α (HIF-1 α), vascular endothelial growth factor (VEGF), and matrix metalloproteinases (MMP)-9 in liver cancer [4].

To this end, this study was conducted to investigate the changes of blood flow signal in residual cancer after RFA treatment of rabbit liver cancer over time (0 h to 2 weeks), and to analyse the correlation between changes in blood flow signal and changes in HIF-1 α , VEGF, and MMP-9 in residual cancer tissue after RFA. The results lay a foundation for the study of medication targets for the treatment of local tumour recurrence after RFA.

MATERIALS AND METHODS

Animal model

One hundred and ten randomly selected New Zealand white rabbits of clean grade (6–7 months old, male or female, 2300 g) from the Animal Centre of Inner Mongolia Medical University were used. VX2 tumour cells supplied by Peking Union Medical College were implanted subcutaneously in the outer thigh of 5 rabbits and passaged. After 14–28 days, tumours growing at the implant site were dissected layer by layer and preserved. Next, the tumours were cut into 1-mm³ pieces under sterile conditions and placed in 0.9% physiological saline. The tumour pieces were

ground and suspended separately, stored in a refrigerator at –80°C for 24 h, and then stored in liquid nitrogen. One hundred and five randomly selected rabbits were fixed on the operating table after anaesthesia via ear vein. Their abdominal cavity was opened by conventional operation of the right rib arch to expose the liver. Next, the liver was obliquely punctured with ophthalmic surgical forceps, implanted with the passaged tumour cells, and stuffed with surgical gelatin sponge. Afterwards, the abdomen was closed layer by layer. Ultrasound examination of tumour growth was performed after 60 days of feeding. Rabbits that suffered from surgical death and infection were excluded according to experimental requirements. The experimental rabbits were observed for general condition. The diameter of the implanted tumours was measured using a real-time colour Doppler ultrasound diagnostic system, Logiq-E8-Face, with a probe frequency of 3.0–5.0 MHz. Five of the rabbits were sacrificed and pathological sections of liver cancer were prepared to observe the pathological changes.

Ethics approval and consent to participate

The present study was approved by the Ethics Committee of the Affiliated Hospital of Inner Mongolia Medical University. Cell studies were approved by the Committee on the Ethics of Animal Experiments of the Affiliated Hospital of Inner Mongolia Medical University.

Evaluation of angiogenesis and blood flow signal in residual cancer after RFA and surgical resection in rabbits with liver cancer

A total of 90 randomly selected rabbits with liver cancer were divided into three groups. Group 1 consisted of 10 untreated controls. Group 2 consisted of 40 rabbits treated with RFA with 10% residual tumour and subdivided into four groups (each of 10 rabbits): 0 hours after treatment, 3 days after treatment, 7 days after treatment, and 14 days after treatment. Group 3 consisted of 40 rabbits treated with surgical resection with 10% residual tumour and subdivided into four groups (each of 10 rabbits): 0 hours after treatment, 3 days after treatment, 7 days after treatment, and 14 days after treatment. For Group 2, after insertion of the RFA electrode into the liver tumour area, eccentric ablation was performed for 4 min at a power of 5 to 50 W. The system was automatically shut down when the impedance reached 100%. 10% of the tumour was left *in situ*. Afterwards, the electrode was removed and the abdomen was closed. Anti-inflammatory treatment was

given. Group 3 underwent conventional liver tumour resection with 10% residual tumour. Afterwards, the abdomen was closed and anti-inflammatory treatment was given. The dynamic changes of microangiogenesis in residual cancer were examined by contrast-enhanced ultrasound in the three groups of rabbits 0, 3, 7 and 14 days after treatment. The ultrasound was performed on each rabbit with all the same parameters (mechanical index, gain, and depth). Tumour size and blood flow signal were evaluated by ultrasound examination. The blood flow signal was classified into four grades: grade 0 — no blood flow signal; grade 1 — sporadic star-shaped blood flow signal; grade 2 — continuous stripe-shaped blood flow signal, representing continuous blood flow activity; and grade 3 — presence of large vessels with a fast blood flow rate.

The contrast agent used was Sonovuc (Bracco, Italy) and administered at the manufacturer's recommended dose. The radiofrequency system used was an RFA treatment system with a double electrode configuration and a power of 50–60 Hz from Covidien (US).

Relationship between blood flow signal and angiogenesis in residual cancer after RFA and surgical resection in rabbits with liver cancer

Rabbits in the control, RFA, and surgical resection groups were sacrificed at the selected time points for tumour tissue sampling. One part of the collected tissue was stained and counted for microvessel density (MVD) in liver cancer; and the others were preserved in liquid nitrogen and embedded in paraffin separately.

Microvessels were counted according to the MVD staining method proposed by Wendy. Brownish yellow staining of the interstitial substance indicated positive cells. Cell masses near the positive staining were vessels. Vessels were counted under low magnification in three selected fields with a relatively dense distribution. The mean \pm standard deviation was calculated.

The expression of VEGF and MMP-9 in liver cancer was measured using the SP method. Rabbit polyclonal antibodies were used for the staining of VEGF and MMP-9. The embedded tissue was sectioned, washed 3 times with phosphate buffered saline (PBS), blocked with hydrogen peroxide for 10–15 min, and antigen-retrieved by high pressure and high temperature. Afterwards, the sections were cooled, washed 3 times with PBS, blocked with serum, and incubated for 15 min at 26°C. Next, VEGF and MMP-9 primary antibodies were added, followed by incubation for 2 h at 37°C, and then secondary antibodies were

added, followed by incubation for 15 min at room temperature. After washing with PBS, the sections were incubated with SP solution for 15 min at room temperature, then washed 3 times with PBS. Next, the sections were developed with DAB solution, washed with running water, then stained with haematoxylin, and observed under microscope. Furthermore, the sections were incubated with rabbit polyclonal antibodies against VEGF and MMP-9 for 1 h at room temperature. At 1–5 min after addition of substrate (Abeam, Cambridge, UK), the sections were counterstained with haematoxylin, dehydrated, and mounted with coverslips. The results of immunohistochemistry were determined according to the instructions of VEGF and MMP-9 assay kits used, which describe VEGF and MMP-9 as localised in the cytoplasm. Five high-power fields were randomly selected for each slide using the image analysis software to determine the average optical density and for statistical analysis.

Correlation of HIF-1 α , VEGF, MMP-9 mRNA and protein expressions with blood flow signal in residual cancer after RFA and surgical resection in rabbits with liver cancer

First, 100 mg of liver cancer tissue samples from each rabbit were homogenised with 1 mL of Trizol reagent (Invitrogen, Carlsbad, CA, USA). Total mRNA was isolated using Trizol reagent. Next, the RNA was redissolved. The RNA pellet was dried. The RNA sample was partially dissolved, triturated 5 times in RNase-free water, incubated at 55–60°C for 10 min, redissolved with 100% formamide, and stored at –70°C. Real-time quantitative polymerase chain reaction (RT-qPCR) was used to quantify HIF-1 α , VEGF, and MMP-9 mRNA levels. The SYBR PrimeScript RT-qPCR kit (TaKaRa, Tokyo, Japan) was used. β -actin was used as an internal control. Primers used were as follows: for HIF-1 α , 5'-GTCGGACAGCCTCACAAACAGAGC3'' (sense) and 5'-GTAACTTGATCCAAAGCTCTGAG-3' (antisense); for VEGF, 5'-CCCTGATGAGATCGAGTACATCTT-3'' (sense) and 5'-ACCGCCTCGGCTrGTCAC-3' (antisense); for MMP-9, 5'-CGGCCACGAGGAACAAACT-3'' (sense) and 5'-CGGAGCACGGAGACGGGTAT3' (antisense); and for β -actin, 5'-TTCTACAATGAGCTGCGTGTG-3' (sense) and 5'-GGGGTGTGAAGGTCAAA-3' (antisense).

All primers were synthesised by Beijing Bioengineering Technology Co., Ltd. (Shanghai, China). The expression levels of HIF-1 α , VEGF, and MMP-9 were expressed as a fold increase from the control, β -actin, and calculated using the $\Delta\Delta$ Ct method.

The protein levels of HIF-1 α , VEGF, and MMP-9 of selected tissue samples were analysed by Western blotting. Tumour samples were homogenised prior to protein isolation. The homogenised samples were collected and dissolved using a bacteriolytic agent (Pierce, Rockford, IL, USA). A protease inhibitor cocktail (Thermo Fisher Scientific, Waltham, MA, USA) was added according to the manufacturer's instructions. Protein samples were separated on a 12% polyacrylamide gel and transferred to a nitrocellulose membrane. HIF-1 α , VEGF, MMP-9, and β -actin were quantified by electrochemiluminescence (Amersham, Uppsala, Sweden) using polyclonal antibodies against rabbit HIF-1 α , VEGF, MMP-9, and β -actin, respectively, and then a peroxidase-conjugated secondary antibody (Sigma, St. Louis, MO, USA).

RESULTS

Of the 105 experimental rabbits, 4 died due to surgical infection, surgical errors, or unknown reasons; and 101 survived after tumour implantation. However, hyperechoic tumour was not observed in the liver by ultrasound in 3 of the surviving rabbits. The reason for this might be surgical errors or inactivation of the implanted tumour tissue. The remaining 98 surviving liver tumour-bearing rabbits had a tumour size of 2.3 ± 0.32 cm (Fig. 1). Ultrasound revealed an intact capsule, high echo of the tumour parenchyma, and mostly wide, but occasionally narrow, surrounding dark halos. The main reason for this was that the tumour pushed away the surrounding small vessels and became surrounded by them. There were no obvious changes in echo intensity in the posterior aspect of liver tumour nodules in most cases. Posterior enhancement was occasionally seen. Masses were observed in adjacent tissues in a few animals.

Five liver tumour-bearing rabbits were randomly selected and sacrificed. There was no difference in morphology between the harvested histopathological sections of liver cancer. Cancerous changes in liver cells were observed in all specimens, exhibiting apparent pathomorphology of liver cancer, often accompanied by megakaryocytes and multinuclear tumour cells. The nuclei were of different size, shape and staining properties. The chromatin was mostly unevenly distributed coarse granules. The nuclear membrane was thick, the nucleus divided, the nuclear division asymmetric, and the cytoplasm mostly basophilic (Fig. 2).

Immediately after ablation, echoes from microbubbles, with an unclear boundary, were detected around



Figure 1. Removed tumour implant from hind limb.

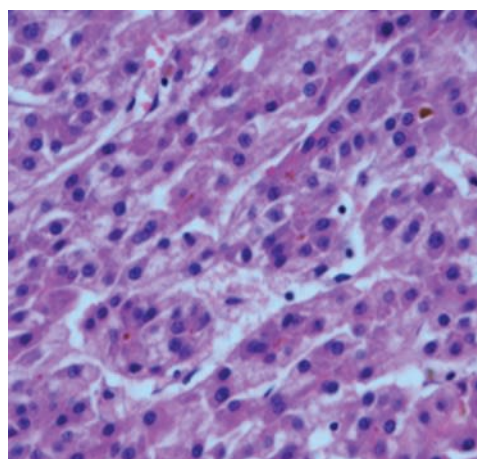


Figure 2. Haematoxylin and eosin staining of rabbit liver cancer tissue (SP \times 200).

the ablation zone. Grade 1 blood flow signals were detected, i.e., almost no blood flow could be detected. Three days after ablation, tumour boundary and size were similar to those before ablation. The boundary was unclear. The ablation zone was hyperechoic. Grade 1 blood flow signals were detected, representing almost no blood flow. The remaining 98 surviving liver tumour-bearing rabbits had a tumour size of 2.3 ± 0.32 cm. Ultrasound revealed an intact capsule in almost all animals, high echo of the tumour parenchyma, and mostly wide, but occasionally narrow, surrounding dark halos. The main reason for this was that the tumour pushed away the surrounding small vessels and became surrounded by them. There were no obvious changes in echoes in the posterior aspect of liver tumour nodules in most cases. Posterior enhancement was occasionally seen. Masses were observed in

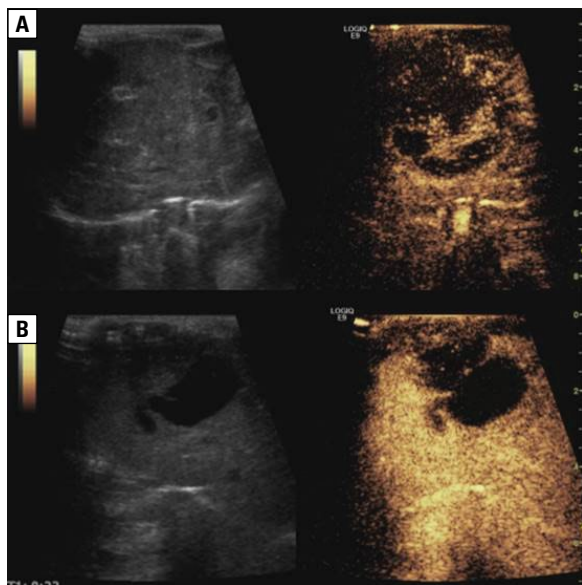


Figure 3. Ultrasound of rabbit liver cancer before and after radiofrequency ablation (RFA); **A.** Before RFA; **B.** After RFA.

adjacent tissues in a few animals (Fig. 3). Ultrasound performed from 7 to 14 days revealed an increasingly clear boundary, high or mixed medium-high echoes in the ablation zone, and blood flow signals of grades 2 and 3. Before treatment, there was no significant difference in the grade of blood flow signal between the control (n = 10), RFA (n = 40), and surgical resection (n = 40) groups (p > 0.05). After treatment, significant differences in the grade of blood flow signal were noted in the surgical resection group between different time points (days 0, 3, 7, and 14) (p < 0.05). Significant differences were also observed between the surgical resection and RFA groups at the same time points (p < 0.05). The blood flow signal intensity in the RFA group was lower than that in the control group, but higher than that in the surgical resection group.

Before RFA, as revealed by contrast-enhanced ultrasound, the contrast around the liver cancer rapidly increased for 5–8 s, and disappeared approximately 20 s later. At 0 and 3 days after RFA, blood flow signals appeared around the tumour, and a defect was present in the liver cancer area 15 s after contrast injection; and no blood flow signal was observed within the tumour. Blood flow enhancement occurred in the previous blood flow defect area in 2 animals on day 7 and in 4 animals on day 14. Similarly, at 0 and 3 days after surgical resection, blood flow signals appeared around the tumour, and a defect was present in the liver cancer area 15 s after contrast injection; and no blood flow signal was observed within the tumour. Blood flow enhance-

Table 1. Vascular grade in three groups before and after radiofrequency ablation (RFA)

Group		Number	Grade 0	Grade 1	Grade 2	Grade 3
Control	Before RFA	10	2	3	5	0
	After RFA		2	3	2	3
RFA group	Before RFA	40	8	14	5	
	0 days after RFA	10	7	2	1	0
	3 days after RFA	10	5	3	2	0
	7 days after RFA	10	4	3	2	1
	14 days after RFA	10	3	4	2	1
Surgical resection group	Before resection	40	9	13	6	0
	0 days after resection	10	8	1	1	0
	3 days after resection	10	7	2	1	0
	7 days after resection	10	6	4	0	0
	14 days after resection	10	6	4	0	0

ment occurred in the previous blood flow defect area in 1 animal on day 7 and in 2 animals on day 14. Significant differences were observed between the surgical resection and RFA groups at the same time points (p < 0.05).

Pathological observation after RFA revealed that the tissue in the ablation zone was mostly necrotic, with dark blue pyknotic nuclei, fragmented chromatin, dissolved nuclear membrane, no visible nuclear boundary, and swelling and liquefaction of the intercellular substance. At 7 and 14 days after RFA, liquefaction occurred in the ablation zone, the necrosis was extended, and fibrosis occurred around the liquefied area (Fig. 1, Table 1).

Intratumoural microvessel density in control, RFA (four subgroups), and surgical resection (four subgroups) groups

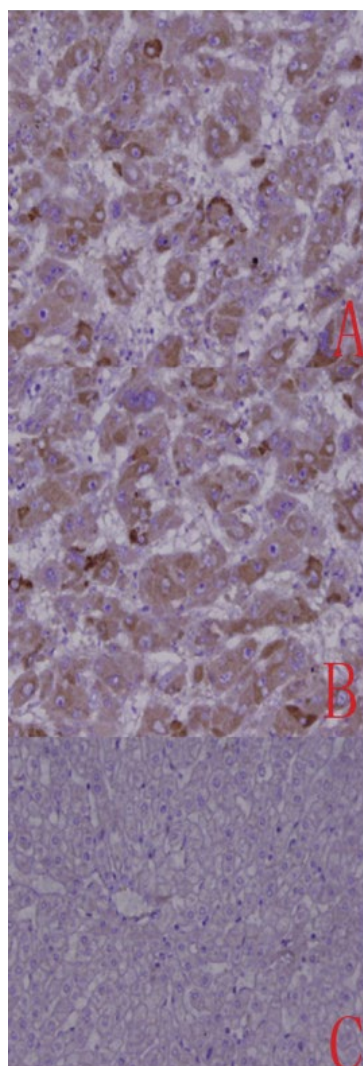
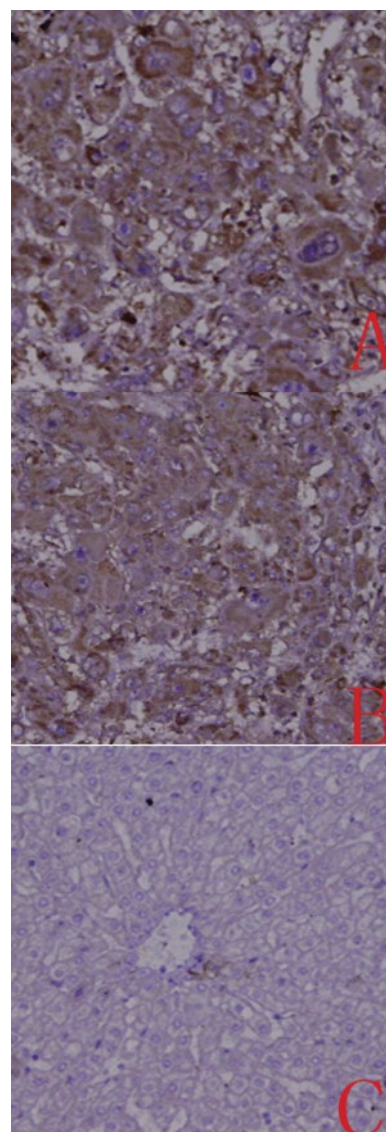
The intratumoural MVD was 32.3 ± 2.3 in the control group. In the RFA group, the MVD was 10.3 ± 3.5 on day 0, 11.4 ± 2.8 on day 3, 17.3 ± 3.1 on day 7, and 31.5 ± 2.2 on day 14. In the surgical resection group, the MVD was 9.8 ± 2.4 on day 0, 9.8 ± 3.4 on day 3, 10.4 ± 1.9 on day 7, and 18.6 ± 2.1 on day 14. Analysis of variance indicated p < 0.05, representing significant differences between groups. Significant differences were also observed between the surgical resection and RFA groups at the same time points (p < 0.05). The MVD in the RFA group was lower than that in the control group, but higher than that in the surgical resection group.

Table 2. Vascular endothelial growth factor (VEGF), and matrix metalloproteinase 9 (MMP-9) expression in each group

Group	VEGF	MMP-9
Control group	67.3 ± 2.46	63.5 ± 2.45
Radiofrequency ablation group:		
Day 0	15.3 ± 0.44	23.6 ± 0.70
Day 3	16.7 ± 0.33	26.5 ± 0.45
Day 7	34.9 ± 1.61	37.3 ± 0.93
Day 14	57.6 ± 0.53	61.5 ± 0.70
Surgical resection group:		
Day 0	16.8 ± 0.72	22.7 ± 0.69
Day 3	15.2 ± 0.75	23.6 ± 0.48
Day 7	26.6 ± 0.66	28.6 ± 0.65
Day 14	35.2 ± 0.72	39.6 ± 0.96

Comparison of VEGF and MMP-9 expression between control, RFA (four subgroups), and surgical resection (four subgroups) groups

Vascular endothelial growth factor and MMP-9 expression in the control, RFA (four subgroups), and surgical resection (four subgroups) groups is shown in Table 2. Analysis of variance gave $F = 2973.896$, $p < 0.05$ for VEGF expression, and $F = 2275.421$, $p < 0.05$ for MMP-9 expression, both representing significant differences between groups. Significant differences were also observed between the surgical resection and RFA groups at the same time points ($p < 0.05$). The immunohistochemical scores for VEGF (Fig. 4) and MMP-9 (Fig. 5) in the RFA group were

**Figure 4.** Vascular endothelial growth factor (VEGF) protein expression in liver cancer (SP × 400); **A, B.** VEGF-positive cells; **C.** VEGF-negative cells.**Figure 5.** Matrix metalloproteinase 9 (MMP-9) protein expression in liver cancer (SP × 400); **A, B.** MMP-9-positive cells; **C.** MMP-9-negative cells.

lower than those in the control group, but higher than those in the surgical resection group.

Correlation of blood flow signal with VEGF and MMP-9 expression and MVD

In the control group, the blood flow signal was positively correlated with the VEGF and MMP-9 expression and the MVD, with correlation coefficients of 0.521, 0.768, and 0.814, respectively (all $p < 0.05$). The blood flow signal was positively correlated with the VEGF and MMP-9 expression and the MVD in both the RFA and surgical resection groups at all time points; in other words, the higher the blood supply grade, the higher the VEGF and MMP-9 expression and MVD. At later time points (days 7 and 14), both the VEGF and MMP-9 expression and the MVD were higher with RFA than with surgical resection.

DISCUSSION

Radiofrequency ablation is a minimally invasive, non-surgical technique in which a needle- or catheter-type electrode is inserted into tumour to produce heat (100–110°C) with a 460 kHz radiofrequency current to kill tumour cells [5]. Ultrasound-guided RFA has been shown to control liver cancer and relieve the symptoms to some extent in clinical research. Ultrasound contrast agents used in recent years combined with high-resolution ultrasound can effectively monitor the properties and development of residual cancer after liver cancer ablation or surgical resection, providing an important basis for timely follow-up [6].

High-resolution ultrasonography was performed after ablation in this study. Immediately after ablation, echoes from microbubbles, with an unclear boundary, were detected around the ablation zone. Grade 1 blood flow signals were detected, representing almost no blood flow. Three days after ablation, tumour boundary and size were similar to those before ablation. The boundary was unclear. The ablation zone was hyperechoic. Grade 1 blood flow signals were detected, representing almost no blood flow. Ultrasound performed from 7 to 14 days revealed an increasingly clear boundary, high or mixed medium-high echoes in the ablation zone, and blood flow signals of grades 2 and 3. From the above results, it is clear that the liver tissue of the untreated control group had relatively high blood flow rates and metabolic activity. In the RFA group, necrosis occurred in the liver cancer tissue due to damage caused by radiofrequency hyperthermia at early time points after RFA. However, at later time points, the liver

cancer tissue that was not damaged by radiofrequency hyperthermia continued to proliferate and undergo malignant change, leading to recurrence of liver cancer. In the surgical resection group, the blood flow in cancer decreased initially, but increased over time, similar to that observed with RFA. However, the blood flow rate was lower with surgical resection than with RFA at the same time points. It indicates that surgical resection can effectively reduce cancer recurrence compared with RFA.

Microvessel density is a relatively accurate indicator for determining local microangiogenesis. It is commonly used for local detection of tumours to determine the nature and recurrence of tumours.

Vascular endothelial growth factor is also known as vascular permeability factor. It can be divided by structure and function into VEGF-A, -B, -C, -D, -E and -F [7]. It is a vital factor during vessel growth and development, promoting the growth and division of vascular endothelial cells [8]. VEGF can induce endothelial cell proliferation and cause increased permeability, leading to vascular oedema and inflammation. The main role of VEGF is to regulate vascular permeability and promote the formation of fibre networks by vascular endothelial cells. In vitro, it can also promote proliferation, differentiation, migration, and adhesion of vascular endothelial cells, as well as matrix degradation, and activate bone marrow-derived endothelial progenitor cells. Liver cancer is a highly vascularised tumour. The hepatic artery provides the main source of blood supply to tumour cells. Liver cancer cells and tumour infiltrating inflammatory cells secrete VEGF, bFGF, PDGF, and some factors that promote neovascularisation and vessel maturation [9]. Clinical studies suggest that VEGF can predict the prognosis of liver cancer [10]; VEGF expression in patients with liver cancer was negatively correlated with their overall survival; and blocking tumour angiogenesis may therefore be a potential target for treatment of liver cancer [11].

Metalloproteinases participate in histogenesis and organ development, and are closely related to tumourigenesis, cardiovascular diseases and central nervous diseases, mainly by affecting the extracellular matrix [12]. MMP-9 belongs to the second major category of MMPs, gelatinase. It is the enzyme with the largest molecular weight in the MMP family. It consists of three α -helices and five beta-sheets, containing two zinc ions and five calcium ions. In its structure, small molecule compounds, which are tightly bound to zinc ions, can be seen at the active centre. MMP-9 is generally detected by zymography [13]. The

main steps of zymography are as follows: 1) separate the sample by SDS-polyacrylamide gel electrophoresis, 2) restore the activity of MMP-9 in the divalent metal ion buffer, 3) stain the gel after electrophoretic separation with Coomassie blue, 4) destain the gel, and 5) observe the bands in a blue background. The intensity of the bands reflects the activity of MMP-9. Therefore, measurement of MMP-9 is important for reflecting the level of angiogenesis [14].

In this study, the blood flow signal was positively correlated with the VEGF and MMP-9 expression and the MVD in both the RFA and surgical resection groups; that is to say, the higher the blood flow signal grade, the higher the VEGF and MMP-9 expression and MVD. At later time points (days 7 and 14), both the VEGF and MMP-9 expression and the MVD were higher with RFA than with surgical resection. The results of this study demonstrate that the ultrasound blood flow signal is associated with the expression of two angiogenesis-related factors, VEGF and MMP-9, and the MVD in the control, RFA, and surgical resection groups. This is consistent with the observations regarding blood flow signals and contrast-enhanced ultrasound findings described in section 'Results'. It indicates that there is a higher risk of tumour recurrence with RFA than with surgical resection. The possibility of tumour recurrence after RFA can be assessed by measurement of VEGF and MMP-9 in clinical practice.

CONCLUSIONS

Radiofrequency ablation can partially destroy tumours. However, the blood flow signal intensity was higher with RFA than with surgical resection at later time points after treatment.

The grade of ultrasound blood flow signal was positively correlated with the expression of two angiogenesis-related factors, VEGF and MMP-9, and the MVD in the control, RFA, and surgical resection groups.

Funding

Inner Mongolia natural science foundation (2016mslh0814).

REFERENCES

1. Abu-Hilal M, Primrose JN, Casaril A, et al. Surgical resection versus radiofrequency ablation in the treatment of small unifocal hepatocellular carcinoma. *J Gastrointest Surg.* 2008; 12(9): 1521–1526, doi: [10.1007/s11605-008-0553-4](https://doi.org/10.1007/s11605-008-0553-4), indexed in Pubmed: [18592325](https://pubmed.ncbi.nlm.nih.gov/18592325/).
2. Chen XY, He QY, Guo MZ. XAF1 is frequently methylated in human esophageal cancer. *World J Gastroenterol.* 2012; 18(22): 2844–2849, doi: [10.3748/wjg.v18.i22.2844](https://doi.org/10.3748/wjg.v18.i22.2844), indexed in Pubmed: [22719195](https://pubmed.ncbi.nlm.nih.gov/22719195/).
3. Huang J, Yan L, Cheng Z, et al. A randomized trial comparing radiofrequency ablation and surgical resection for HCC conforming to the Milan criteria. *Ann Surg.* 2010; 252(6): 903–912, doi: [10.1097/SLA.0b013e3181efc656](https://doi.org/10.1097/SLA.0b013e3181efc656), indexed in Pubmed: [21107100](https://pubmed.ncbi.nlm.nih.gov/21107100/).
4. Huang J, Yao Wy, Zhu Qi, et al. XAF1 as a prognostic biomarker and therapeutic target in pancreatic cancer. *Cancer Sci.* 2010; 101(2): 559–567, doi: [10.1111/j.1349-7006.2009.01396.x](https://doi.org/10.1111/j.1349-7006.2009.01396.x), indexed in Pubmed: [19922503](https://pubmed.ncbi.nlm.nih.gov/19922503/).
5. Kempkensteffen C, Fritzsche FR, Johannsen M, et al. Down-regulation of the pro-apoptotic XIAP associated factor-1 (XAF1) during progression of clear-cell renal cancer. *BMC Cancer.* 2009; 9: 276, doi: [10.1186/1471-2407-9-276](https://doi.org/10.1186/1471-2407-9-276), indexed in Pubmed: [19664236](https://pubmed.ncbi.nlm.nih.gov/19664236/).
6. Kubo H, Hayashi T, Ago K, et al. Temporal expression of wound healing-related genes in skin burn injury. *Leg Med (Tokyo).* 2014; 16(1): 8–13, doi: [10.1016/j.legalmed.2013.10.002](https://doi.org/10.1016/j.legalmed.2013.10.002), indexed in Pubmed: [24269074](https://pubmed.ncbi.nlm.nih.gov/24269074/).
7. Morimoto M, Numata K, Kondou M, et al. Midterm outcomes in patients with intermediate-sized hepatocellular carcinoma: a randomized controlled trial for determining the efficacy of radiofrequency ablation combined with transcatheter arterial chemoembolization. *Cancer.* 2010; 116(23): 5452–5460, doi: [10.1002/cncr.25314](https://doi.org/10.1002/cncr.25314), indexed in Pubmed: [20672352](https://pubmed.ncbi.nlm.nih.gov/20672352/).
8. Rossi S, Ravetta V, Rosa L, et al. Repeated radiofrequency ablation for management of patients with cirrhosis with small hepatocellular carcinomas: a long-term cohort study. *Hepatology.* 2011; 53(1): 136–147, doi: [10.1002/hep.23965](https://doi.org/10.1002/hep.23965), indexed in Pubmed: [20967759](https://pubmed.ncbi.nlm.nih.gov/20967759/).
9. Szymczak AL, Workman CJ, Wang Y, et al. Correction of multi-gene deficiency in vivo using a single 'self-cleaving' 2A peptide-based retroviral vector. *Nat Biotechnol.* 2004; 22(5): 589–594, doi: [10.1038/nbt957](https://doi.org/10.1038/nbt957), indexed in Pubmed: [15064769](https://pubmed.ncbi.nlm.nih.gov/15064769/).
10. Volin MV, Koch AE. Interleukin-18: a mediator of inflammation and angiogenesis in rheumatoid arthritis. *J Interferon Cytokine Res.* 2011; 31(10): 745–751, doi: [10.1089/jir.2011.0050](https://doi.org/10.1089/jir.2011.0050), indexed in Pubmed: [21864160](https://pubmed.ncbi.nlm.nih.gov/21864160/).
11. Vordenbäumen S, Sewerin P, Lögters T, et al. Inflammation and vascularisation markers of arthroscopically-guided finger joint synovial biopsies reflect global disease activity in rheumatoid arthritis. *Clin Exp Rheumatol.* 2014; 32(1): 117–120, indexed in Pubmed: [24387883](https://pubmed.ncbi.nlm.nih.gov/24387883/).
12. Wang J, Gu Q, Li M, et al. Identification of XAF1 as a novel cell cycle regulator through modulating G(2)/M checkpoint and interaction with checkpoint kinase 1 in gastrointestinal cancer. *Carcinogenesis.* 2009; 30(9): 1507–1516, doi: [10.1093/carcin/bgp155](https://doi.org/10.1093/carcin/bgp155), indexed in Pubmed: [19628579](https://pubmed.ncbi.nlm.nih.gov/19628579/).
13. Wang M, Tan J, Wang Y, et al. IL-18 binding protein-expressing mesenchymal stem cells improve myocardial protection after ischemia or infarction. *Proc Natl Acad Sci USA.* 2009; 106(41): 17499–17504, doi: [10.1073/pnas.0908924106](https://doi.org/10.1073/pnas.0908924106), indexed in Pubmed: [19805173](https://pubmed.ncbi.nlm.nih.gov/19805173/).
14. Yang WT, Chen DL, Zhang FQ, et al. Experimental study on inhibition effects of the XAF1 gene against lung cancer cell proliferation. *Asian Pac J Cancer Prev.* 2014; 15(18): 7825–7829, doi: [10.7314/apjcp.2014.15.18.7825](https://doi.org/10.7314/apjcp.2014.15.18.7825), indexed in Pubmed: [25292071](https://pubmed.ncbi.nlm.nih.gov/25292071/).